International Journal of Automotive Technology, Vol. 16, No. 3, pp. 525–537 (2015)
DOI 10.1007/s12239–015–0054–x

pISSN 1229–9138/ eISSN 1976–3832

PROTOTYPE VARIABLE TRANSMISSION SYSTEM FOR ELECTRIC VEHICLES: ENERGY CONSUMPTION ISSUES

P. SPANOUDAKIS* and N. C. TSOURVELOUDIS

Department of Production Engineering and Management, Technical University of Crete, Chania 73100, Greece

(Received 17 October 2013; Revised 23 January 2014; Accepted 29 January 2014)

ABSTRACT–In order to explore the performance of variable transmission use on zero emission urban vehicles, targeting low fuel consumption, a new type of a flat-belt driven CVT was developed. The new Electronic Shift Variable Transmission (ESVT) was build in order to be installed and tested on the ER12 prototype hydrogen fuel cell powered urban vehicle, which is developed by the TUC Eco Racing team at the Technical University of Crete. ER12 is used as a testbed vehicle in order to measure fuel consumption and compare results of ESVT use versus the one-stage geared transmission that was previously installed on the vehicle. At first, a description of the proposed system main components and design considerations is presented, in order to provide insight on system operation. Actual road tests are conducted using the prototype vehicle, providing insights regarding fuel consumption measurements and driving performance with and without ESVT. Experimental results are presented, showing significant improvement with the use of the proposed system. ESVT control logic analysis follows, describing the control objectives and rules used towards lower fuel consumption and driving performance. Finally, evaluation of ESVT control operation is presented, using experimental results from the road tests conducted with ER12 prototype vehicle.

KEY WORDS : CVT, Powertrain, Flat belt, Fuel consumption, Zero emission, Electric vehicle

1. INTRODUCTION

After more than a century of research and development, the Internal Combustion (IC) engine is near both perfection and obsolescence: engineers continue to explore the outer limits of IC efficiency and performance, but advancements in fuel economy and emissions have effectively stalled (EURONCAP, 2009). While many IC vehicles meet low emissions vehicle standards, these will give way to new, stricter government regulations in the very near future. With limited room for improvement, and given the natural limits of fossil fuels, automobile manufacturers have begun full-scale development of alternative power vehicles. Thus, other vehicle types are researched and produced towards zero emissions goal, like electric and fuel cell powered vehicles. At the same time, efficiency of every engine and power transmission components are explored in order to achieve lower fuel consumption and higher autonomy. Nowadays much focus has been given by the automotive industry on new or optimized powertrain systems that can significantly improve fuel consumption especially in IC engine vehicles.

But since hybrid, fuel cell and electric vehicles are becoming more feasible and promising, such fuel efficient powertrain systems are researched for hybrid/electric cars too (Miller, 2006).

**Corresponding author.* e-mail: hroniss@dpem.tuc.gr

Most current production vehicles use either conventional Manual Transmissions (MTs) with discrete gear ratios or Automatic Transmissions (ATs) configured with planetary gear sets that use integral clutches and bands to change gear ratios. MTs use five to seven discrete gear ratios while ATs have four or five. Alternatively, Continuously Variable Transmissions (CVTs) introduced a totally new infinite gear ratio variation instead of the previously mentioned discrete gear ratio transmissions.

The CVT system was firstly conceptualized by Leonardo Da Vinci at 1490 and installed on a vehicle for the first time at 1910, by Zenith motorcycle manufacturer (Birch, 2000). Although CVTs have been used in automobiles for decades, limited torque capabilities and questionable reliability have inhibited their growth (Kluger and Long, 1999). Nowadays, CVTs are aggressively competing with automatic transmissions and several vehicle manufacturers, are already keen on exploiting the various advantages of a CVT in a production vehicle (Kluger and Long, 1999), (Yamaguchi, 2000).

CVT gear boxes theoretically have an infinite number of transmission ratios, which can be achieved between high and low extremes, with fewer moving parts. The technological advantage is that CVTs change gear ratios at every time instant so as to achieve optimal engine efficiency. This improves the mileage compared to traditional gear boxes by allowing better matching of the engine operating conditions to the variable driving

scenarios.

Several different types of CVTs have been developed through the years, each having their own characteristics. The most referenced types found are: Spherical CVT (Kim *et al*., 2002), Hydrostatic CVT (Lino *et al*., 2005; Kanphet *et al*., 2005), E-CVT (Sakai, 1988; Miller, 2006), Toroidal CVT (Fuchs *et al*., 2002; Tanaka, 2003; Akehurst *et al.*, 2006), Power-split CVT (Mucino *et al*., 2001; Mantriota, 2001; Mantriota, 2005), Belt CVT (Srivastava and Haque, 2009), Chain CVT (Srivastava and Haque, 2009), Ball-type toroidal CVT (Belfiore and De Stefani, 2003), and Milner CVT (Milner, 2002). However, belt and chain types are the most commonly used CVTs, among all, in automotive applications.

The efficiency of manual transmissions, ranges from 96.2% and may be improved up to 96.7% the most. Concerning the overall efficiency of Automatic Transmissions (ATs), it is found to be around 85.3%, whereas the efficiency of the best current AT could be improved up to 86.3% (Vroemen, 2001; Kluger and Long, 1999). At the same time, the overall efficiency of belt type CVTs is estimated at 84.6%, and may be improved towards 88.4% by reducing the pump losses (Vroemen, 2001; Kluger and Long, 1999). These hydraulic pump losses practically determine the efficiency of CVTs and of ATs, and they are relatively high at low transmission loads. The improvement of pump and hydraulic circuit design can substantially increase the efficiency of CVT and AT and it is a subject of ongoing research (Vroemen, 2001). Alternatively, the actuation of the clutches and of the CVT may be (partly) electrical, so as the hydraulic losses to be replaced by potentially lower electrical losses. In (Kluger and Long, 1999; Machida, 1999) the overall efficiency of toroidal or traction drive CVTs is estimated at around 91%, which may become higher by 1.8% by employing more advanced traction fluids.

Almost all studies on CVTs agree that their use may increase the fuel savings and reduce the polluting emissions (Carbone *et al.*, 2007; Brace *et al*., 1999; Brace *et al.*, 1997; Carbone *et al*., 2002; Carbone *et al.*, 2004; Kluger and Fussner, 1997; Boos and Mozer, 1997; Ryu and Kim, 2008). For instance, a mid class CVT car may achieve fuel savings of about 10% in comparison to the traditional manual stepped transmissions (Brace *et al*., 1999; Brace *et al*., 1997; Carbone *et al*., 2002; Carbone *et al.*, 2004). They are also measured to be faster in 0-60 mph acceleration tests (Boos and Mozer, 1997). Moreover their efficiency depends less on driving habit than manual transmissions (Kluger and Fussner, 1997). The potential for fuel efficiency gains can also be seen in the CVT's currently used in several new models that are tested by many automotive magazines (Buyyourcar, 2012).

1.1. Motivation

The relevant literature evident that CVT use has been extensively researched and tested in IC and hybrid vehicles, resulting in reduced fuel consumption. Even though all types of CVTs present different efficiencies, they all exhibit lower consumption than classic manual transmissions, regardless of driving habits. However, to the best of our knowledge, the use of continuous variable transmission has not been researched on zero emission vehicles, such as, electric and hydrogen fuel cell vehicles.

In this work, in order to explore the performance of the variable transmission on zero emission urban vehicles, a flat-belt driven CVT was developed. The new Electronic Shift Variable Transmission (ESVT), targets both efficiency and low fuel consumption and it was developed for the EcoRacer 2012 (ER12) prototype hydrogen fuel cell powered urban vehicle, which is designed by the TUC Eco Racing team of the Technical University of Crete (Efstathiou *et al*., 2012). The ER12 competed in 2012 at the Shell Eco Marathon international fuel consumption competition. It is used as a testbed in order to measure fuel consumption and compare results of ESVT use versus the fixed geared transmission that was previously installed on the vehicle.

Driving performance is another aspect researched. Acceleration time and distance through various speeds is evaluated and compared to one-stage transmission, providing insight on vehicle ability to move better on the road. Both fuel consumption and driving ability using a variable transmission, are tested for the first time on a hydrogen powered vehicle.

In what follows we describe the suggested variable transmission system.

2. ELECTRONIC SHIFT VARIABLE TRANSMISSION

The proposed *Electronic Shift Variable Transmission* (ESVT) consists of a) mechanical components which transmit the power from motor to the wheel and b) electronics, which are responsible for gear ratio change and control. The prototype we present here, was kept simple for weight reduction reasons, however it represents the concept. The total ESVT weight is measured 2.922 Kg. A description of the mechanical and electronic components follows.

2.1. Mechanical Structure

The main mechanical parts for the proposed ESVT system are shown in Figure 1. It mainly consists of two cone pulleys that are connected through a flat belt and are driven by the vehicle electric motor. The movement of the belt on the pulleys provides the change of gear ratio which results to variable power transmission. In our implementation, the belt moves with the aid of a linear actuator driven by the ESVT controller. The output of the ESVT controller is the transmission ratio change, which is implemented through the belt reposition over the cones. In the prototype described here a linear actuator is responsible for the

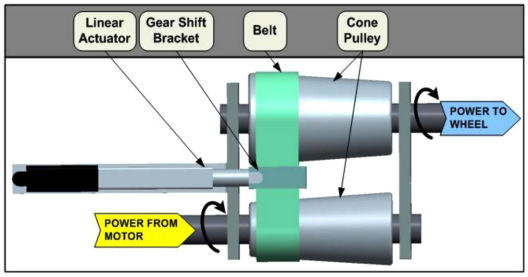

Figure 1. ESVT assembly CAD design.

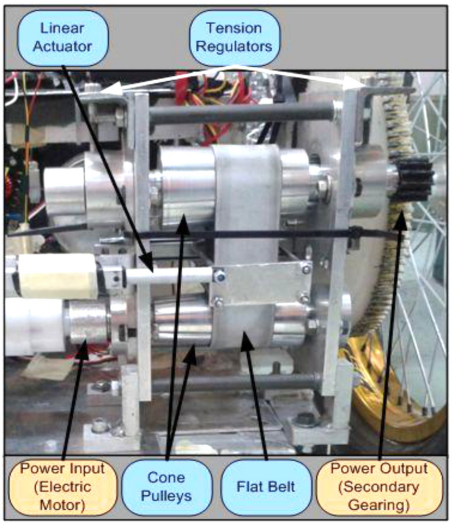

Figure 2. ESVT realization as installed on testbed vehicle.

physical reposition of the belt. Thus, power input is provided by an electric motor to the lower cone pulley, where using a flat belt results to power output transfer from the upper cone pulley axle to the wheel, for vehicle movement. A schematic diagram of the ESVT main components as installed on a vehicle is shown in Figure 2. The two tension regulators on the upper part of the ESVT are used to adjust the belt tension, which is set once before operation.

The transmission system described here was designed and built in order to provide certain capabilities to a specific prototype vehicle, whose objective is the lowest possible fuel consumption. The desired capabilities correspond to higher traction force thus lower consumption at vehicle launch and electronically shifted gear ratio at higher speeds, targeting electric motor best efficiency region. These targets are reached using variable gear ratios ranging from 1.5 to 1 (by the ESVT), which in addition to a fixed secondary gear results to a final drive of 1:15 to 1:10. The secondary gearing is used to raise the torque at the levels needed to move the specific vehicle.

2.2. Control System Electronics

ESVT electronics are responsible for the control of the

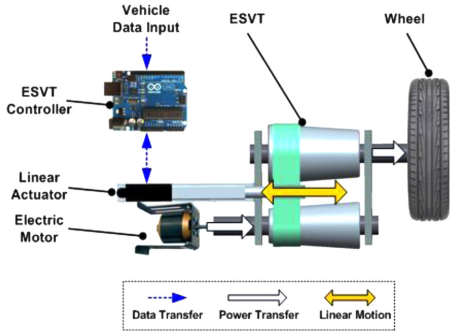

Figure 3. Schematic diagram of the ESVT main components and control system electronics.

variable gear ratio change, which is referred as electronic shift. The control system electronics consist of (Figure 3):

(a) A programmable microcontroller which hosts the software used to process the input signals from sensors and compute the appropriate output. *Vehicle speed*, *Current actuator position, Throttle, Motor speed and Speed change* are the main inputs and *Actuator move* is the output. According to input info, the belt move is calculated in order to change ESVT's gear ratio. Detailed info regarding ESVT control logic are provided at paragraph 5.1.

(b) A linear actuator used to move the belt to a new position (i.e. change ESVT gear ratio), according to controller output. The new belt position corresponds to a new gear ratio.

All input-output data are transferred via a mini motherboard to an SSD drive, where they are recorded during operation for evaluation purposes.

3. DESIGN CONSIDERATIONS AND THEORY

3.1. Flat Belt Use

3.1.1. Basic geometry considerations

Belts and other similar elastic or flexible machine elements have been widely used to transmit power for a long time. They can be used instead of other rigid power-transmission devices as gears and in many cases their use simplifies the design and reduces the cost (Shigley and Mischke, 1989). The power is transmitted from the driver pulley to the driven pulleys through friction between the belt and the pulleys. Belt drives can absorb shock loads and damp out vibration effects which is an important advantage for any machine's life. There are four principal types of belts which are mainly used: flat, Round, V shaped and timing. The proposed ESVT requires the use of a flat belt, thus flat belt mechanics will be presented hereafter.

Flat belt drives consist of a strong elastic core surrounded by an elastomer and materials vary according to usage. They can provide efficiency up to 98%, close to gear drives, while V-belt drives range from 70–96% (De Almeida and Greenberg, 1995), (Moff, 1989). They also

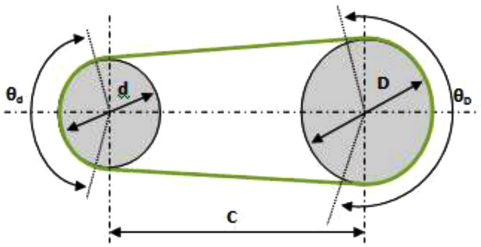

Figure 4. Open belt drive.

produce less noise and absorb more torsional vibration from the system than V-belts or gears.

In a typical open-belt drive as in Figure 4, the small pulley is the driving pulley and the large one the driven. The contact angles are found to be:

$$\theta_d = \pi - 2*sin^{-1}\frac{D-d}{2C} \quad (1)$$

$$\theta_D = \pi + 2*sin^{-1}\frac{D-d}{2C} \quad (2)$$

where, θ_d is the driving pulley contact angle, θ_D is the driven pulley contact angle, D is the diameter of driven pulley, d the diameter of driving pulley and C is the center distance of pulleys.

The length of the belt is found by summing the two arc lengths between twice the distance of the beginning and end of contact which results to:

$$L = [4C^2 - (D-d)^2]^{1/2} + \frac{1}{2}(D\theta_D + d\theta_d) \quad (3)$$

This equation can be simplified to the following equation used by all belt manufacturers for the length calculation:

$$L \approx 2C + \frac{\pi}{2}(D+d) + \frac{(D-d)^2}{4C} \quad (4)$$

3.1.2. Belt tensions

According to literature (Mantriota, 2005), (Shigley and Mischke, 1989), a change in belt tension due to friction forces between the belt and pulley will cause the belt to elongate or contract and move relative to the surface of the pulley. This motion is caused by elastic creep and is associated with sliding friction as opposed to static friction. The action at the driving pulley, through that portion of the angle of contact that is actually transmitting power, is such that the belt moves more slowly than the surface speed of the pulley because of the elastic creep. The angle of contact consists of the effective arc, where power is transmitted, and the idle arc. The belt first contacts the driving pulley with a tight-side tension F_1 and a velocity V_1, which is the same as the pulley surface velocity. Then, belt passes through the idle arc with no change in F_1 or V_1. Creep or sliding contact follows, and the belt tension changes in accordance with the friction forces. At the end of the effective arc the belt leaves the pulley with a loose-side tension F_2 and a reduced speed V_2.

In Figure 5, the free body diagram of a small segment of the belt is presented both in 2D and 3D perspectives. Assuming that the friction force on the belt is uniform throughout the entire arc of contact, the belt segment is subjected to a *centrifugal force F_C, a normal force between the belt and pulley dN, and a friction force ìdN* at the point before slip occurs.

The length of the belt segment results to,

$$dl = r\, d\theta \quad (5)$$

where, r the pulley radius and $d\theta$ the contact arc on pulley.

The centrifugal force is,

$$F_C = (mrd\theta)r\omega^2 = mV^2 d\theta \quad (6)$$

where, V is the belt speed, r the pulley radius and m is the belt mass per unit length equal to,

$$m = bt\rho \quad (7)$$

where, b is the width, t is the thickness and ρ is the density of the belt material.

From the equation of equilibrium in the tangential and radial direction,

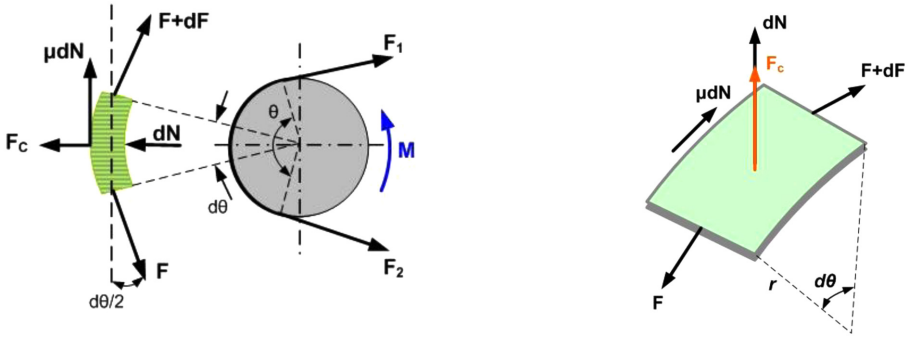

Figure 5. Free body diagram of a belt small segment.

$$\Sigma F_t = 0 \Rightarrow$$
$$F\cos\frac{d\theta}{2} - (F+dF)\cos\frac{d\theta}{2} + \mu dN = 0 \Rightarrow \quad (8)$$
$$dF = \mu dN$$

$$\Sigma F_r = 0 \Rightarrow$$
$$F_C + dN - F\sin\frac{d\theta}{2} - (F+dF)\sin\frac{d\theta}{2} = 0 \quad (9)$$

where, F is the belt tension force, F_C the centrifugal force, dN the reaction force, μdN the friction force, μ the coefficient of friction and $d\theta$ the contact arc on pulley.

For a small angle $d\theta$ it can be assumed that,

$$\cos\frac{d\theta}{2} \cong 1 \text{ and } \sin\frac{d\theta}{2} \cong \frac{d\theta}{2} \quad (10)$$

Then, from (9) and using (6), (8),

$$mV^2 d\theta + \frac{1}{\mu}dF - Fd\theta - dF\frac{d\theta}{2} = 0 \quad (11)$$

Since $d\theta/2$ is really small compared to the other quantities of the equation, it becomes,

$$mV^2 d\theta + \frac{1}{\mu}dF - Fd\theta = 0$$
$$\Rightarrow \frac{dF}{F - mV^2} = \mu d\theta \quad (12)$$

Considering the entire angle of wrap,

$$\int_{F_1}^{F_2} \frac{dF}{F - mV^2} = \int_0^{\theta} \mu d\theta$$
$$\Rightarrow \frac{F_1 - mV^2}{F_2 - mV^2} = e^{\mu\theta} \quad (13)$$

where, F_1 is the belt tension force on tight-side, F_2 the belt tension force on loose-side, μ the coefficient of friction, θ the effective contact arc on pulley, V is the belt speed, m is the belt mass per unit length.

Thus, the final equation for the determination of relationship between belt tensions is,

$$\frac{F_1 - F_C}{F_2 - F_C} = e^{\mu\theta} \quad (14)$$

where, F_1 is the belt tension force on tight-side, F_2 the belt tension force on loose-side, F_C the centrifugal force, μ the coefficient of friction and θ the effective contact arc on pulley.

If an initial tension F_i is set to the belt as an added constraint during belt installation, then tension equations transform to:

$$F_1 = F_i + F_C + \Delta F = F_i + F_C + \frac{M}{D} \quad (15)$$

$$F_2 = F_i + F_C - \Delta F = F_i + F_C - \frac{M}{D} \quad (16)$$

where, ΔF is tension due to transmitted torque M and D pulley diameter.

Solving for the initial tension provides the equation that defines the maximum belt tension:

$$F_i = \frac{F_1 + F_2}{2} - F_C \quad (17)$$

In equation (17) the maximum belt tension will occur when $F_1 = 2F_i$. Thus the only way to transmit more power is to increase the initial belt tension. Based on that, the belt drive is designed for the maximum tension F_1 which is limited according to the allowable tension specified by the belt manufacturer (size, material etc).

3.1.3. Linear actuating force derivation

The linear force (F_A) needed to provide horizontal belt movement, which corresponds to ESVT gear ratio change, is derived hereafter. This actuating force is needed in order to choose a suitable linear actuator, capable to move the flat belt during operation of the proposed ESVT (Spanoudakis, 2013). To our knowledge no other theory was found in literature to calculate this force on such a prototype transmission system. Figure 6 shows the forces acting on the belt when it is moved along the cone pulleys.

In order to proceed to linear actuating force calculation, the following assumptions are made: *a)the belt does not deform due to F_A having nearly rigid body motion relative to the pulleys, b)belt move is opposed by kinetic friction and c)the cone angle of the conical pulleys is too small thus the belt is on total contact in all directions on the pulleys.*

From the equation of equilibrium in the horizontal direction (Figure 6a) we obtain:

$$F_A = T_D + T_d \quad (18)$$

where, T_D and T_d are the friction force at driven and driving pulley respectively.

Choosing a small belt segment (Figure 6b) at one of the pulleys (driving) and according to the equilibrium of forces at the direction of dF_A, results to,

$$dF_{Ad} = \mu dN_d \quad (19)$$

where, dF_{Ad} is the linear actuating force on small belt segment contacting the driving pulley, dN_d the reaction force on small belt segment contacting the driving pulley and μ the coefficient of friction.

Using (19) and (8) is found that:

$$dF_{Ad} = dF \Rightarrow F_{Ad} = \int_{F_2}^{F_1} dF \Rightarrow$$
$$F_{Ad} = (F_1 - F_2) \Rightarrow F_{Ad} = 2\Delta F \quad (20)$$

Also, from (14), using (15), (16) and substituting at (17),

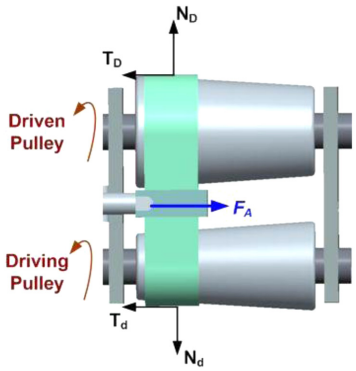

(a)

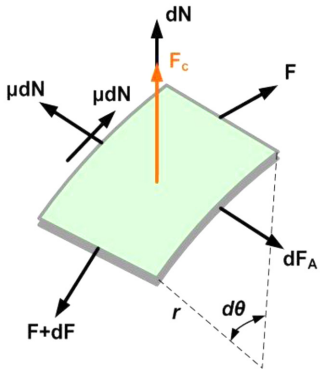

(b)

Figure 6. (a) Free body diagram of belt acting forces during ratio change; (b) Free body diagram of a belt small segment during ratio change.

results that:

$$\Delta F = \frac{M}{d} = F_i \frac{e^{\mu\theta_d} - 1}{e^{\mu\theta_d} + 1} \tag{21}$$

where, ΔF is tension due to transmitted torque M and d the driving pulley diameter.

Thus using (20) and (21), the linear actuating force at one pulley is found:

$$F_{Ad} = 2F_i \frac{e^{\mu\theta_d} - 1}{e^{\mu\theta_d} + 1} \tag{22}$$

Finally, the required linear actuating force needed to move the belt horizontally, can be calculated from (21) and (22), resulting to:

$$F_A = 2F_i \left(\frac{e^{\mu\theta_d} - 1}{e^{\mu\theta_d} + 1} + \frac{e^{\mu\theta_D} - 1}{e^{\mu\theta_D} + 1} \right) \tag{23}$$

In order to compute F_A, it is needed to measure the initial tension set, as also the geometries of the cone pulleys which result to contact angles calculation. It is important to note that during belt movement kinetic friction coefficient (μ_K) is applied, instead of static friction coefficient used at (14).

3.1.4. Linear actuating force calculation

According to the previously derived equations, the linear actuating force (F_A) is calculated for the proposed ESVT.

Basic system geometry data used are:

C = 86 mm
d = 34.67 mm
D = 52 mm
F_i = 70 N
μ_s = 0.6
μ_k = 0.5

Initial tension F_i was measured using a mechanical tension meter, applied at the belt while the ESVT was setup for road test operation. Also, the static (μ_s) and kinetic (μ_k) coefficients of friction were found from flat belt manufacturers manuals, for polyurethane flat belt on aluminum pulleys (Gates Mectrol, 2008).

According to the above, it is found that using Equation (1), (2) results to:

θ_d = 168 (deg)
θ_D = 192 (deg)

Using Equation (23) results to F_A calculation, which is found F_A = 183.34N.

According to this value, a linear actuator capable to provide forces up to 200N was chosen and installed on the ESVT.

3.1.5. Flat belt tracking

Tracking effects like angled pulleys and idlers as well as conical pulleys were mostly known by experience (Egger and Hoffman, 2012). Nevertheless, the axial motion of a flat belt, as also the belt and pulley properties that influence that motion should be taken in account. Several researchers (Gerbert, 1999) derived some basic equations and calculated some preliminary results of flat belts, running on conical pulleys. Other theoretical and experimental analysis of flat belt tracking due to angled axis and crowned pulleys were also found at (Egger and Hoffman, 2007; Egger and Hoffman, 2011).

It can be observed that flat belts, supported and driven by cylindrical pulleys are subject to no guiding force. They may run in an unstable condition and flat belt pulleys need to be carefully aligned to prevent the belt from moving off. Guiding systems can generally be separated in two basic physical principles for steering flat belts: a) *Form conditioned* where the steering effect relies on geometry and normal forces and b) *Force conditioned* where steering effect relies on contact load and friction. In the later principle, in conical tail pulley use, the belt moves towards the largest diameter during operation. This effect applies on the described ESVT system.

3.1.6. Flat belt tracking on the ESVT

In every case found in literature, research has been done if one of the two pulleys is conical (tail pulley), but no

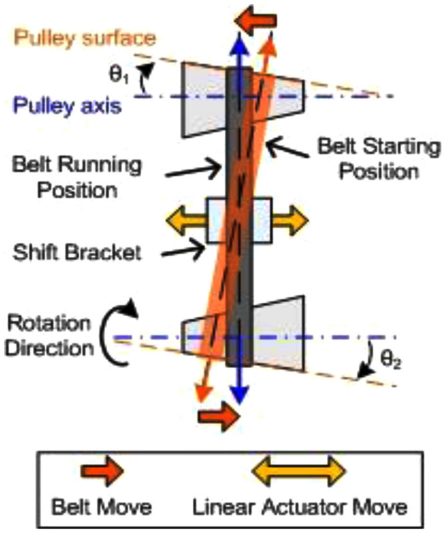

Figure 7. Flat belt axial movement on the two conical pulleys of the ESVT.

research have been found to compensate for double conical pulley use. When both pulleys are conical, like in the proposed prototype ESVT, similar axial belt movements occur. Specifically, when the belt is firstly installed, its center line is vertical to the cone outer surface (Figure 7). Both conical pulleys are constructed and placed with the same cone angle (θ_1=θ_2) even though they have different diameters, thus the belt is vertical to both pulley surfaces. When the pulleys start to rotate, a double axial movement effect is produced, forcing the belt to running position. As described before, this is caused as the belt tends to move to higher diameters. At that position the belt center line becomes almost vertical to the pulleys rotation axes. In order to keep the belt at a specific position, a gear shift bracket moved by the linear actuator, provides the exact ratio change between pulleys.

3.1.7. CVT ratio change

A continuously variable transmission (CVT) has a gear ratio that can be varied continuously within a certain range, providing an infinity of gear ratios (Ehsani *et al*., 2005). This continuous variation allows for the matching of virtually any engine speed and torque to any wheel speed and torque. It is therefore possible to achieve an ideal torque–speed profile (constant power profile), because any engine power output to the transmission can be applied at any speed to the wheels.

At the proposed ESVT concept, the distance between the two pulleys remains constant while the belt is moved along the pulley axis, varying the effective diameter on which the belt grips. The transmission ratio (i_g) is a function of the two effective diameters:

$$i_g = \frac{D}{d} \tag{24}$$

where, D and d are the effective diameters of the output pulley and input pulley, respectively.

3.1.8. Motor efficiency measurement

As already stated, our main purpose is to use the proposed ESVT in order to reduce fuel consumption by using variable transmission advantages, one of which is electric motor operation at maximum efficiency. In order to achieve that, motor maximum efficiency must be reached at specifc rpm. Since no data were available from the manufacturer, an efficiency testbed was developed. The main target was to measure the specific electric motor maximum efficiency at specific loads, which corresponds to vehicle operation at the target speed of 25 Km/h. At that speed the needed power to move the vehicle is calculated at $P_{25\,Km}$=200 W (Spanoudakis, 2013). Thus, experimental measurements were conducted for this specific external load at various motor speeds and maximum efficiency was obtained.

The efficiency testbed (Figure 8) consists of a *rotary torque transducer* connected to the *electric motor* axle (input) and to a *hydraulic disc brake* (output), measuring: Motor speed (Rpm), Torque (Nm) and Power (Kw). External load is applied through the hydraulic disc brake, regulated at 200 W for all experimental measurements.

Electric motor speed is regulated using a speed controller and torque measurements are recorded every 500 Rpm. The torque transducer data are used as output data, compared to input data collected from amperometer and voltmeter measurements, which are directly connected to the motor input.

Motor efficiency is then calculated using equation (25) and is presented at Figure 9 (Vroemen, 2001).

$$n_t = \frac{P_{out}}{P_{input}} \times 100 \tag{25}$$

where, P_{out} is the power output provided to the wheels and

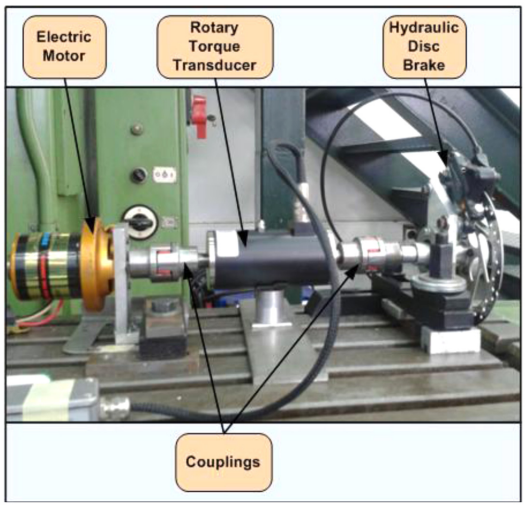

Figure 8. Developed testbed used to measure motor efficiency.

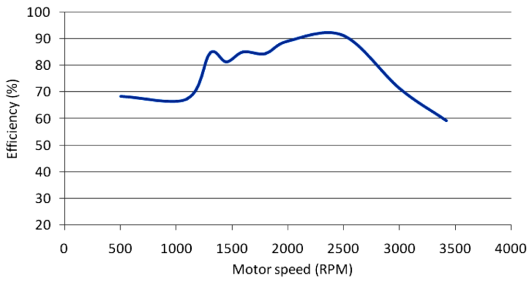

Figure 9. Motor efficiency measurements versus motor speed at 200W external load.

P_{in} the power input of the electric motor, and n_t is given as a percentage.

Experimental results showed that maximum motor efficiency (91.3%) is reached at 2500 RPM. Also revealed that an optimal RPM range of motor operation is from 2300 to 2500 Rpm, where efficiency exceeds 90%. According to these valuable info, the ESVT control must be regulated to provide gear ratios that will operate the vehicle motor at this range.

3.2. ESVT Control Logic

The ESVT control main target is to continuously approximate an optimal ESVT gear ratio, according to vehicle power demands (Spanoudakis, 2013). This is translated to linear actuator movement control (i.e. belt movement on the cone pulleys), which results to ratio change. The optimal gear ratio (r_{opt}) is met when the electric motor is operated inside its maximum efficiency region (>90%), found at 2300–2500 Rpm (paragraph 3.1.8). At this speed, lowest energy consumption of the testbed vehicle is achieved.

For the decision of the new gear ratio, the controller uses five inputs and based on IF-THEN rules one output is extracted (Figure 10). The control inputs are: 1)Vehicle velocity *(Velocity)*, 2)Current actuator position (*sensor_value*), 3)Throttle Position (*throttle*), 4)Motor Speed (*Motor_Rpm*), 5)Velocity Change (*Vel_change*) and the output is: 1)Actuator move (*Forward*, *Backward or Stop)*. Control inputs 1-3 are sensor inputs, while control inputs 4, 5 are calculated using the first three inputs.

According to vehicle speed input and current actuator position, the current gear ratio (r_{cur}) and then current *motor Rpm* is calculated. To obtain r_{cur}, it is assumed that *gear ratio (r)* changes between *sensor_value* max-min positions, following a linear function: r_{cur} =a*sensorValue+b, where a, b are constants. The max-min ESVT gear ratios and actuator positions are: $1.5 > r > 1.0$ and $850 > sensorValue > 600$, respectively. Solving for r and *sensorValue* limits, results to a, b calculation and Equation (26) is extracted, providing the current gear ratio (r_{cur}).

$$r_{cur} = 0.00146 sensor\_value + 0.2604 \quad (26)$$

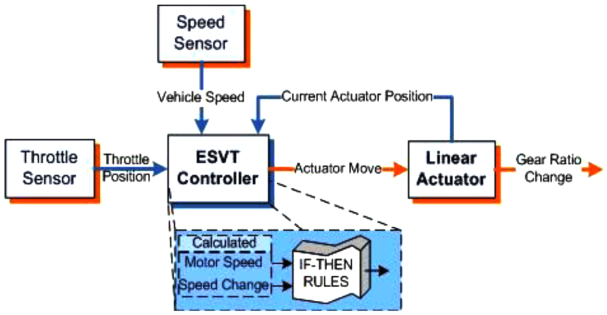

Figure 10. ESVT control architecture.

Wheel speed (Rpm) is calculated by (27):

$$Wheel\ speed(Rpm) = \frac{velocity}{\pi d_w}\frac{1000}{60} \quad (27)$$

where, *velocity* is vehicle's velocity (km/h) and d_w the wheel diameter.

Between the wheel and the ESVT, a secondary gearing (ratio 1:10) exists. Thus motor speed is:

$$Motor\_Rpm = Wheel\ speed\ 10r \quad (28)$$

Using (27) and (28) results to:

$$Moter\_Rpm = 9.828\ velocity\ 10\ r \quad (29)$$

According to (29), motor speed is calculated at all times using the velocity and gear ratio control inputs.

Speed change is also calculated using the velocity input, in order to define vehicle acceleration or deceleration:

$$Vel\_change = Velocity_{new} - Velocity_{old} \quad (30)$$

Motor speed and Speed change values are used as additional calculated inputs throughout the IF-THEN rules, in order to obtain control output.

A total of eight (8) IF-THEN rules are used to control linear actuator motion, as presented at Table 1. There, IF statements correspond to the five control input variables and THEN statements to the one control output. The darker shaded cells at IF statements are the calculated input variables whilst the rest are sensors input. Every variable considered at an IF statement is marked with an X, while at output, green cells show actuator move and red cells actuator stop.

The generic control rule of ESVT operation is the following:

GENERIC RULE

IF *velocity* is A AND *Motor_Rpm* is B AND *Throttle* is C THEN *actuator* moves backward.

As an example consider the explanation of rule (5):

IF *velocity>15 Km/h* AND *Motor_Rpm<2300* AND

Table 1. ESVT control rules definition.

RULES	IF												THEN		
	VELOCITY			VELOCITY CHANGE	MOTOR RPM			ACTUATOR CURRENT POSITION			THROTTLE		ACTUATOR MOVE		
	<5	5-15	>15	<-3	<2300	2300-2500	>2500	<850	START=850	END=650	>0	0	FORWARD	BACKWARD	STOP
1	X														
2		X						X							
3		X							X						
4			X				X			X					
5			X		X							X			
6			X			X									
7			X				X				X				
8			X	X							X				

Throttle=0 THEN *actuator must move backward*. At this case, the vehicle is assumed to decelerate. Thus, higher gear ratios should be achieved (actuator backward move), providing higher torque capabilities in order to accelerate again when throttle is pressed.

As shown, rules 1, 2 and 4, serve mainly as operational limits, while the rest (3 and 5-8) are used to approximate optimal motor operation. As already stated, the main target is to achieve motor operation near its best efficiency region, set at 2300–2500 RPM.

At the same time, the optimal gear ratio must be achieved with the fewer possible belt movements. That way, higher belt service life and ESVT efficiency is expected, avoiding additional belt wear and power loss respectively.

4. ENERGY CONSUMPTION RESULTS

4.1. Testbed Vehicle

In order to evaluate the transmission system through on road experimental testing, the prototype urban vehicle ER12 is used (Figure 11).

It is a one seat, low weight vehicle for urban environments, developed by the Technical University of Crete Eco Racing team (TUCER) (Efstathiou *et al*., 2012). An electric motor powered from a H_2 fuel cell, make up the vehicle's energy system. The basic powertrain consists of a one-stage geared transmission with ratio 1:10, placed between the electric motor and the wheel. Testbed technical specifications are presented at Table 2. The vehicle weight (excluding the driver) is measured at 81 kg without the ESVT, while with the ESVT installed it is found 84 Kg.

Figure 11. Prototype testbed vehicle ER12.

Table 2. Testbed technical specifications.

Chassis	Aluminum alloy
Body	Carbon fiber
Motor	Brushless electric motor
Max motor torque	4 Nm
Max motor RPM	4000 RPM
Power source	H_2 fuel cell, 1.2 KW
Dimensions	2.5 × 1.25 × 1m (L × W × H)
Weight	81 Kg
Max vehicle speed	37 Km/h

4.2. Fuel Consumption

The main purpose of this paper is to evaluate ESVT use, according to fuel consumption measurements. The prototype vehicle ER12 was used at different driving conditions and the results were evaluated in contrast to the basic vehicle transmission installation with fixed gear ratio.

The fixed one-stage gear transmission has a constant ratio 1:10 (one (1) wheel rotation corresponds to ten (10) rotations of the electric motor). When the ESVT is used, it is placed before the 1:10 gearing, resulting in variable ratios 1:10r1:15.

An open test track at the University campus was used for the tests, where one full lap corresponds to 240 m. The tests were conducted firstly without the use of the ESVT, measuring: *time, distance, vehicle velocity and hydrogen consumption*. Then, ESVT was installed and the same tests were conducted again in order to compare fuel consumption data.

Two major test cases were investigated. One, conducting acceleration tests of 0–25 Km/h and another completing one full lap corresponding to 240 m distance. At both cases full throttle was used.

It must be stated that the testbed vehicle is developed for competition purposes, where an average speed of 25 Km/h

is the target. That is the reason why this specific speed is used throughout the tests.

4.2.1. Testcase 1 (Acceleration 0-25 Km/h)

Acceleration is the most fuel consuming driving condition, which becomes really important while using vehicles at urban environments. Thus, it is crucial to evaluate whether the use of the proposed ESVT results in better hydrogen consumption while accelerating from stop to the target speed of 25 km/h. At the same time, the driving performance is investigated in order to evaluate if the vehicle can reach the speed of 25 km/h with the ESVT installed.

At this test the vehicle is accelerated at full throttle, which corresponds to acceleration pedal maximum position. On road tests are conducted with and without the use of the ESVT. The results of velocity measurements and hydrogen consumption are shown in Figures 12 (a), 12 (b) respectively.

As seen on Figure 12 (a), the vehicle reached the target speed at a longer distance when using the ESVT (ESVT: 68.14 m, No ESVT: 60.49 m). Nevertheless the calculated average velocity was slightly higher with the ESVT (ESVT: 10.33 Km/h, No ESVT: 9.89 Km/h). This is explained due to the difference of starting transmission ratios (ESVT: 1:15, No ESVT: 1:10), where ESVT provides higher acceleration up to 12 km/h. Above that speed, ESVT ratio changes slow down vehicle acceleration, mostly due to friction losses that occur from belt movement. Hence, velocity comparison measurements show that with the ESVT the driving performance of the vehicle is improved.

Fuel consumption measurements (Figure 12 (b)), show a lower hydrogen consumption using ESVT (*1.33lt*), compared to No ESVT (*1.66lt*), which corresponds to a **19.9%** improvement. Also, as shown, hydrogen consumption is lower throughout the vehicle acceleration, as expected from the less stepped velocity measurements that occur using the ESVT. Since hydrogen consumption is a key factor for evaluating ESVT use, it is clear that it allows lower consumption during acceleration. In urban environments where many stop and go are needed, this will result in higher fuel savings which is the main target.

4.2.2. Testcase 2 (One lap)

In order to evaluate vehicle driving and consumption regarding the proposed ESVT use, additional tests were conducted. For this testcase the prototype vehicle should complete one full lap inside the test track. More specifically, the vehicle must start from zero speed, accelerate, decelerate for the first corner, accelerate again, decelerate for the second turn and finish. This test was made in order to correspond to real driving conditions.

Once again tests are firstly performed without the ESVT and then ESVT installation and testing follows. Also for this case the vehicle is driven at full throttle during accelerations in order to obtain more adequate results. The measurements of vehicle velocity and hydrogen consumption are shown in Figures 13 (a), 13 (b) respectively, as a comparison between ESVT and No ESVT use.

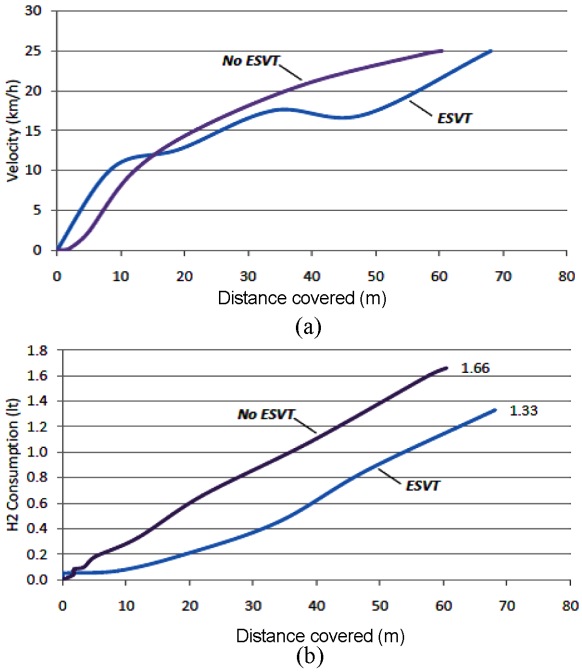

Figure 12. (a) Vehicle velocity comparison when accelerating 0-25 km/h; (b) Vehicle velocity and hydrogen consumption when accelerating 0-25 km/h.

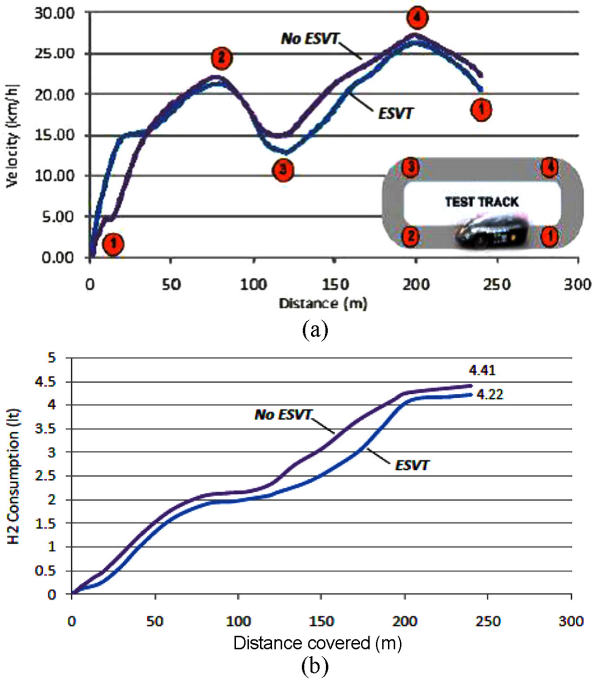

Figure 13. (a) Vehicle velocity comparison driving 1 lap; (b) Hydrogen consumption comparison at 1 lap.

Figure 13 (a) presents the vehicle velocity comparison (ESVT, No ESVT) as also the test track including four specific waypoints, in order to be clear where every acceleration and deceleration occurs. Velocity measurements show that without the ESVT the vehicle obtained a higher maximum velocity (ESVT: 25.5 Km/h, No ESVT: 27.3 Km/h). Nevertheless, the average velocity was higher when using the ESVT (ESVT: 15.7 Km/h, No ESVT: 13.9 Km/h). It should be noticed though, that the drop of speed when decelerating on corners using the ESVT is higher. This is explained due to the higher transmission losses that occur from belt tension, which slow down the vehicle. That is also one reason why the ESVT needs more distance in order to accelerate again at same speeds as with the typical gearing transmission.

Consumption results reveal that ESVT use provides lower hydrogen consumption (ESVT: 4.22lt, No ESVT: 4.41lt), which correspond to a **4.3%** improvement (Figure 13b). Even though not close to the improvement presented during the acceleration tests, it is clear that real road tests prove that ESVT use can lower fuel consumption on an electric vehicle. Even more, one lap test data measurements become more important considering that they correspond to real urban driving conditions.

One lap tests showed that using the ESVT results in more stable vehicle driving on track, since variable transmission ratios provide smoother acceleration and deceleration transactions. That, allows the driver to optimize its driving performance easier and thus achieve even better consumption results as he gets to know the vehicle. Even though without the ESVT a higher maximum speed can be obtained, it should be accounted that the test track has really short straights where the vehicle can't show its real potentials. It is important that in competition tracks (for which it is built), longer straight parts are available thus it is easier to achieve higher maximum speeds resulting to also higher average speeds.

Also, since the ratio changes are user programmed, vehicle average speed can be optimized for every different track needs. That is an important advantage of ESVT use that cannot be achieved with direct one-stage gear transmission.

4.3. ESVT Control Results

In order to explore and evaluate ESVT control operation, experimental data of actuator movements were recorded, during 1)acceleration and 2)one lap test cases. Graphical representations of these data are shown at Figures 14, 15. ESVT belt position is also presented schematically at specific ratio change points to clarify ESVT operation.

4.3.1. Testcase 1 (Acceleration 0-25 Km/h)

For the first test case, experimental data of vehicle velocity and ESVT ratio are presented at Figure 14.

At start, transmission ratio remains at 1:1.5 up to 16 km/h, where it starts to change in order to help on reaching higher vehicle speeds. As shown, ratio changes are done with smooth transitions, resulting to good vehicle acceleration. Between 17–18 Km/h, quick ratio change (1:1.5 to 1:1.3) requires quick belt movement and thus higher transmission losses occur. This sudden power loss results to vehicle speed drop. Above 18 Km/h, smooth gear shift resumes smooth vehicle acceleration up to the target speed. Hence, during acceleration tests ESVT control operation is evaluated as good, since there are no sudden ratio changes and the small lag presented at 17–18 Km/h was expected according to ESVT mechanical construction.

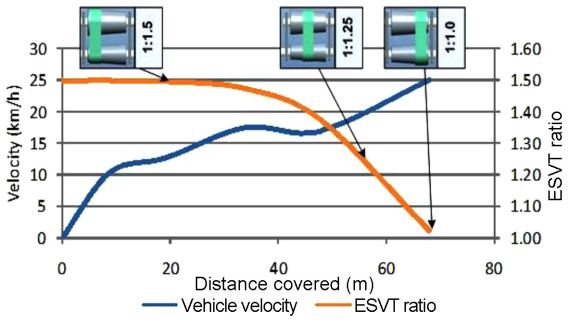

Figure 14. Vehicle velocity and ESVT gear ratio during acceleration test.

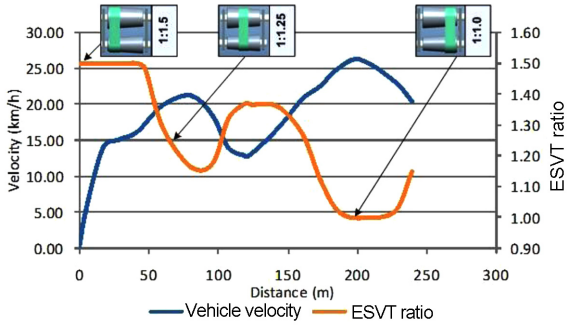

Figure 15. Vehicle velocity and ESVT gear ratio during one lap test.

4.3.2. Testcase 2 (One lap)

For the second test case, the experimental data representing vehicle velocity and ESVT ratio are presented at Figure 15. As shown, ESVT ratio remains at 1:1.5 until vehicle reaches 16 km/h and then it moves to lower ratios. The small hysteresis of vehicle acceleration that is evident at this point (15–17 Km/h) is expected due to high gear ratio used. Once the ratio starts to change, the vehicle accelerates again up to 22 Km/h. It is important that for the rest of the track, the control responds to vehicle speed changes, providing ratios that can keep the needed speed and torque. Also, smooth ratio transitions seem to follow the target of low belt movement in order to avoid high power losses.

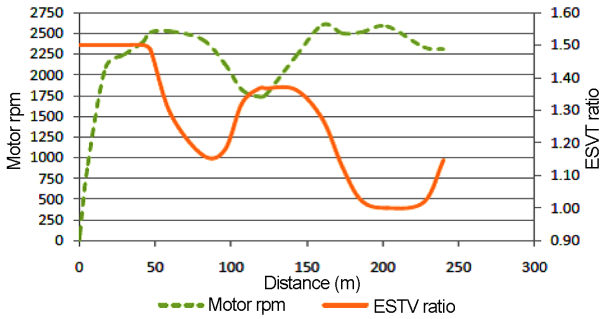

Figure 16. Motor RPM and ESVT gear ratio during one lap test.

While the above findings are important, mostly for the vehicle driving performance, the key factor of ESVT use towards higher fuel autonomy, *is to keep motor speed closely to best motor efficiency region (2300–2550Rpm)*. To evaluate this operational characteristic, ESVT ratio versus motor speed is presented at Figure 16.

According to the specific vehicle application (i.e gear ratios), best motor efficiency region can only be achieved at speeds over 17 km/h. There, it is possible according to vehicle speed to operate the motor near this Rpm region. As viewed, during vehicle launch (40–80 m of the covered distance), ESVT control clearly follows this key rule, trying to keep almost constant motor Rpm even though the vehicle accelerates and decelerates. This operation is repeated during 150–220 m of the covered distance, where once the motor speed exceeds the 2500 Rpm limit, the control rules are followed towards motor speed drop to efficiency region. Also, the constant ratio sections found, prove that low actuator movements are succeeded, which is the second control target set.

Experimental results regarding ESVT control evaluation indicate good performance, towards motor operation at best efficiency region speeds. At the same time, smooth ratio transitions occur and are achieved with the fewer possible belt movements, ensuring low belt wear.

5. CONCLUSION

A new prototype Electronic Shift Variable Transmission is presented. The proposed transmission was designed, developed and tested on road, in order to explore the performance of variable transmission use on zero emission urban vehicles. The ESVT was installed and tested on the ER12 prototype hydrogen fuel cell powered urban vehicle. ER12 is used as a testbed in order to measure fuel consumption and compare results of ESVT use versus the one-stage geared transmission previously installed on the vehicle.

Road tests were conducted using the prototype urban vehicle in order to provide insights regarding fuel consumption measurements and driving performance. Experimental results were presented, showing significant improvement with the use of ESVT. Specifically, two major test cases were investigated. One, accelerating the vehicle up to 25 km/h and another completing one full lap while the speed of 25 km/h should be reached. The first case results showed lower hydrogen consumption using ESVT, which corresponds to *19.9%* improvement. At the same time the vehicle reached the target speed at almost the same distance and the average velocity was slightly higher when using the ESVT. Second case results also presented lower hydrogen consumption using ESVT, which corresponds to *4.3%* improvement. Without the ESVT the vehicle obtained a higher maximum velocity, nevertheless the average velocity was slightly higher when using ESVT.

Experimental results regarding ESVT control evaluation indicate good performance, towards motor operation at best efficiency region speeds. At the same time, smooth ratio transitions occur and are achieved with the fewer possible belt movements, ensuring low belt wear.

These insights prove good operational capability of the proposed system. It is also found that future work could focus on ESVT control optimization that can provide even higher fuel consumption improvements and better vehicle drivability.

ACKNOWLEDGEMENT–Many thanks to TUC Eco Racing team members and especially to D. Efstathiou and J. Stratigos.

REFERENCES

Akehurst, S., Parker, D. A. and Schaff, S. (2006). CVT rolling traction drives – A review of research into their design, functionality, and modeling. *ASME J. Mechanical Design* **128**, **5**, 1165–1176.

Belfiore, N. P. and De Stefani, G. (2003). Ball toroidal CVT: a feasibility study based on topology, kinematics, statics and lubrication. *Int. J. Vehicle Design* **23**, **3–4**, 304–331.

Birch, S. (2000). Audi takes CVT from 15th century to 21st century. *Automotive Engineering Int*.

Boos, M. and Mozer, H. (1997). ECOTRONIC – the continuously variable ZF transmission (CVT). *Transmission and Driveline Systems Symp. SAE Paper No.* 970685. 61–67.

Brace, C., Deacon, M., Vaughan, N. D., Horrocks, R. W. and Burrows, C. R. (1999). The compromise in reducing exhaust emissions and fuel consumption from a diesel CVT powertrain over typical usage cycles. *Proc. CVT'99 Cong., Eindhoven*, 27–33.

Brace, C., Deacon, M., Vaughan, N. D., Burrows, C. R. and Horrocks, R. W. (1997). Integrated passenger at diesel CVT powertrain control for economy and low emissions. *ImechE Int. Seminar S540, Advanced Vehicle Transmission and Powertrain Management*.

Buyyourcar (2012). http://www.buyyourcar.co.uk/car-reviews/nissan/micra/micra-12-12v-visia-cvt-5dr/8765

Carbone, G., Mangialardi, L. and Mantriota, G. (2002). Fuel consumption of a mid class vehicle with infinitely variable transmission. *SAE J. Engines* **110**, **3**, 2474–2483.

Carbone, G., Mangialardi, L. and Mantriota, G. (2004). Performance of a city bus equipped with a toroidal traction drive. *IASME Trans*. **1**, **1**, 16–23.

Carbone, G., Mangialardi, L., Bonsen, B., Tursi, C. and Veenhuizen, P. A. (2007). CVT dynamics: Theory and experiments. *Mechanism and Machine Theory*, **42**, 409–428.

De Almeida, A. and Greenberg, S. (1995). Technology assessment: Energy efficient belt transmissions. *Energy and Buildings*, **22**, 245–253.

Efstathiou, D. S., Petrou, A. K., Spanoudakis, P., Tsourveloudis, N. C. and Valavanis K. P. (2012). Recent advances on the energy management of a hybrid electric vehicle. *20th Mediterranean Conf. Control & Automation (MED)*.

Egger, M. and Hoffman, K. (2012). Tracking of flat belts. *J. Mechanics Engineering and Automation*, **2**, 27–36.

Egger, M. and Hoffman, K. (2007). Lateral running of flat belts: The angled conical pulley. *Int. Conf. Mechanism and Machine Science*, *France*.

Egger, M. and Hoffman, K. (2011). Tracking of flat belts by skewing pulley axis. *Int. Conf. Mechanism and Machine Science*, *Mexico*.

Ehsani, M., Gao, Y., Gay, S. E. and Emadi, A. (2005). *Modern Electric*, *Hybrid Electric*, *and Fuel Cell Vehicles: Fundamentals*, *Theory and Design.* CRC Press. London.

EURONCAP (2009). Moving Forward, 2010 - 2015 Strategic Roadmap. EURONCAP Report.

Fuchs, R., Hasuda, Y. and James, I. (2002). Modeling simulation and validation for the control development of a full-toroidal IVT. *Proc. CVT 2002 Cong*., **1709**, 121–129.

Gates Mectrol (2008). Belt Backings – Specifications. Gates Mectrol Inc.

Gerbert, G. (1996). Belt slip–a unified approach. *J. Mechanical Design*, **118**, 432–438.

Gerbert, G. (1999). *Traction Belt Mechanics*. Chalmers University of Technology. Sweden.

Johnson, K. L. (1985). *Contact Mechanics.* Cambridge University Press. Cambridge.

Kanphet, P., Jirawattana, P. and Direcksataporn, B. (2005). Optimal operation and control of a hydrostatic CVT powertrain. *SAE Trans. J. Passenger Cars: Mechanical Systems* **114**, **6**, 1838–1845.

Kim, J., Park, F. C., Park, Y. and Shizuo, M. (2002). Design and analysis of a spherical continuously variable transmission. *ASME J. Mechanical Design* **124**, **1**, 21–29.

Kluger, M. A. and Long, D. M. (1999). An overview of current automatic, manual and continuously variable transmission efficiencies and their projected future improvements. *SAE Paper No.* 1999-01-1259.

Kluger, M. A. and Fussner, D. R. (1997). An overview of current CVT mechanisms, forces and efficiencies. *Transmission and Driveline Systems Symp*. *SAE Paper No.* 970688, 81–88.

Lino, T., Okuda, A., Takano, M., Tanaka, M., Sakai, K., Asano, T. and Fushimi, K. (2005). Research of hydrostatic CVT for passenger vehicles. *JSAE Review* **24**, **3**, 227–230.

Machida, H. (1999). Traction drive CVT up to date. *Proc. Int. Cong. Continuously Variable Power Transmission (CVT'99)*, 71–769.

Mantriota, G. (2001). Theoretical and experimental study of power split continuously variable transmission system: Part I. *Proc. Institution of Mechanical Engineers, Part D: J. Automobile Engineering* **215**, **7**, 837–850.

Mantriota, G. (2005). Fuel consumption of a vehicle with power split CVT system. *Int. J. Vehicle Design* **37**, **4**, 327–342.

Miller, J. M. (2006). Hybrid electric vehicle propulsion system architectures of the e-CVT type. *IEEE Trans. Power Electronics* **21**, **3**, 756–767.

Milner, P. J. (2002). Milner CVT for high torque applications. *Proc. CVT 2002 Cong*., **1709**, 543–554.

Moff, R. (1989). Flat belts. *Machine Design*, 52–70.

Mucino, V. H., Lu, Z., Smith, J. E., Cowan, B. and Kmicikiewicz, M. (2001). Design of continuously variable power split transmission for automotive applications. *Proc. Institution of Mechanical Engineers, Part D: J. Automobile Engineering* **215**, **4**, 469–478.

Ryu, W. and Kim, H. (2008). CVT ratio control with consideration of CVT system loss. *Int. J. Automotive Technology* **9**, **4**, 459–465.

Sakai, Y. (1988). The "Ecvt" electro continuously variable transmission. *SAE Special Publication Papers (PT-125)*. *SAE Paper No.* 880481.

Shigley, J. E. and Mischke, C. R. (1989). *Mechanical Engineering Design*. McGraw-Hill. New York.

Spanoudakis, P. (2013). *Design and Tuning of Operational Parameters for a Prototype Transmission System.* Ph.D. Dissertation, Technical University of Crete. Greece.

Srivastava, N. and Haque, I. (2009). A review on belt and chain continuously variable transmissions (CVT): dynamics and control. *Mechanism and Machine Theory*, **44**, 19–4.

Tanaka, H. (2003). Torque control of a double cavity half-toroidal CVT. *Int. J. Vehicle Design* **32**, **3**–**4**, 208–215.

U.S. Department of Energy (2001). Energy Technology and Fuel Economy. U.S. Department of Energy. U.S. Environmental Protection Agency. http://www.fueleconomy.gov/feg/atv.shtml

Vroemen, B. (2001). *Component Control for the Zero Inertia Powertrain*. Ph. D. Dissertation. Technische Universiteit Eindhoven. Netherlands.

Yamaguchi, J. (2000). Nissan's Extroid CVT. *Automotive Engineering Int.*